Cell Reports, Volume *36*

Supplemental information

Molecular control of cell density-mediated exit to quiescence

Yilin Fan and Tobias Meyer

FigS1

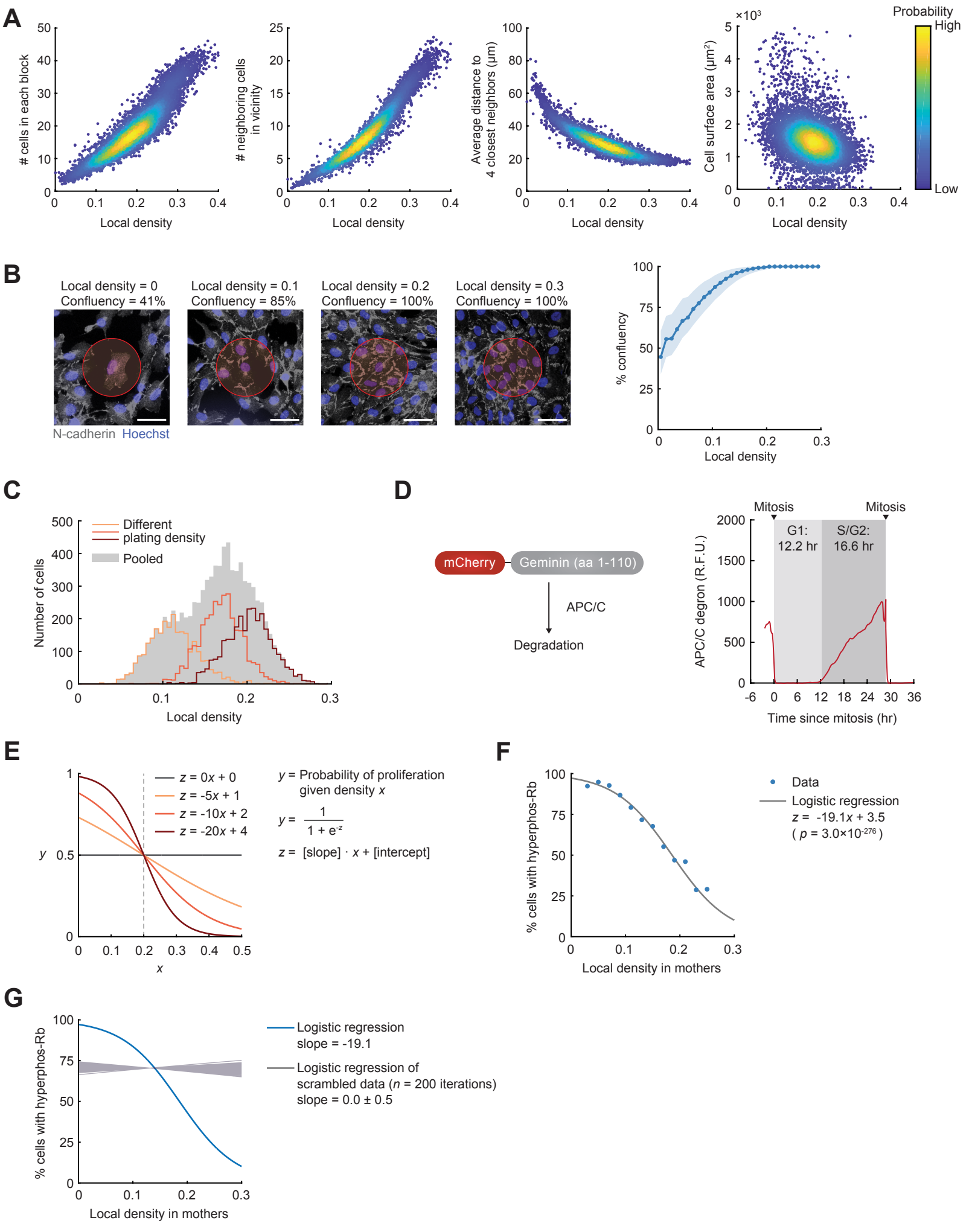
A
cells in each block
Local density
neighboring cells in vicinity
Average distance to 4 closest neighbors (μm)
Cell surface area (μm²)
×10³
Probability
High
Low
B
Local density = 0
Confluency = 41%
Local density = 0.1
Confluency = 85%
Local density = 0.2
Confluency = 100%
Local density = 0.3
Confluency = 100%
N-cadherin Hoechst
% confluency
C
Different plating density
Pooled
Number of cells
D
mCherry
Geminin (aa 1-110)
APC/C
Degradation
Mitosis
Mitosis
G1: 12.2 hr
S/G2: 16.6 hr
APC/C degron (R.F.U.)
Time since mitosis (hr)
E
z = 0x + 0
z = -5x + 1
z = -10x + 2
z = -20x + 4
y = Probability of proliferation given density x
y = 1 / (1 + e^-z)
z = [slope] · x + [intercept]
F
% cells with hyperphos-Rb
Local density in mothers
Data
Logistic regression
z = -19.1x + 3.5
(p = 3.0×10^-276)
G
% cells with hyperphos-Rb
Local density in mothers
Logistic regression slope = -19.1
Logistic regression of scrambled data (n = 200 iterations) slope = 0.0 ± 0.5

Figure S1, related to Figure 1

(A) Local cell density metric (as described in Figure 1A) was correlated with other methods of measuring local cell density. (i) Images were split into 216×216 pixel (134×134 μm) blocks and the number of cells in each block were counted. The cell of interest was subsequently assigned to a block. (ii) The number of neighboring cells (identified by centroid of nuclear marker) with 50 μm of a given cell. (iii) Average distance to 4 closest neighbors (identified by centroid of nuclear marker) of a given cell. (iv) Cell surface area measured by imaging mosaic cultures of non-fluorescent cells and cells expressing a cell surface marker (CaaX-iRFP) (Bisaria et al., 2020). Pearson correlation coefficient = 0.93, 0.97, -0.92, -0.37 ($n \geq$ 2,000 cells per plot).
(B) Left: measuring cell sheet confluency using an antibody specific to N-cadherin. Cell body is masked by thresholding N-cadherin intensity over background. Scale bar: 50 μm. Right: correlation between confluency and local cell density measurement. Shaded error bars are 25^{th}~75^{th} percentile ($n \geq 198$ cells per bin).
(C) Population distributions of local density when cells were plated at different densities (plated at 2.7×10^4 cm^{-2}, 4.0×10^4 cm^{-2}, 5.3×10^4 cm^{-2} one day before imaging). Note the cell-to-cell heterogeneity in local density within the same plating density.
(D) Left: schematic of degron-based APC/C activity reporter. Right: sample trace of asynchronously cycling RPE-1 hTERT cells expressing mCherry-tagged APC/C degron. The boundary of G1/S was identified by the first time that the degron signal exceeds a binary threshold for three consecutive frames.
(E) Schematic of logistic regression applied to the prediction of proliferation given density. A larger negative slope indicates that density is a stronger predictor of proliferation.
(F) Logistic regression of data in Figure 1E. A vector of local density data (each element belonging to a single cell) is used as the predictor, while a vector of 0's and 1's (corresponding to non-proliferating and proliferating cells, as measured by Rb hyperphosphorylation) is used as the response ($n \geq 50$ cells per bin, n = 8,574 cells total). Cross-validation (10-fold) was performed: slope = -19.1 ± 0.1 (median ± s.t.d.), AUC-ROC = 0.74 ± 0.01.
(G) Logistic regression of data in Figure 1E, while scrambling data by randomly matching elements in the predictor vector (density) with elements in the response vector (proliferation status measured by Rb hyperphosphorylation). The logistic regression slope fitted from the original data is unlikely to have resulted from random, spurious correlation.

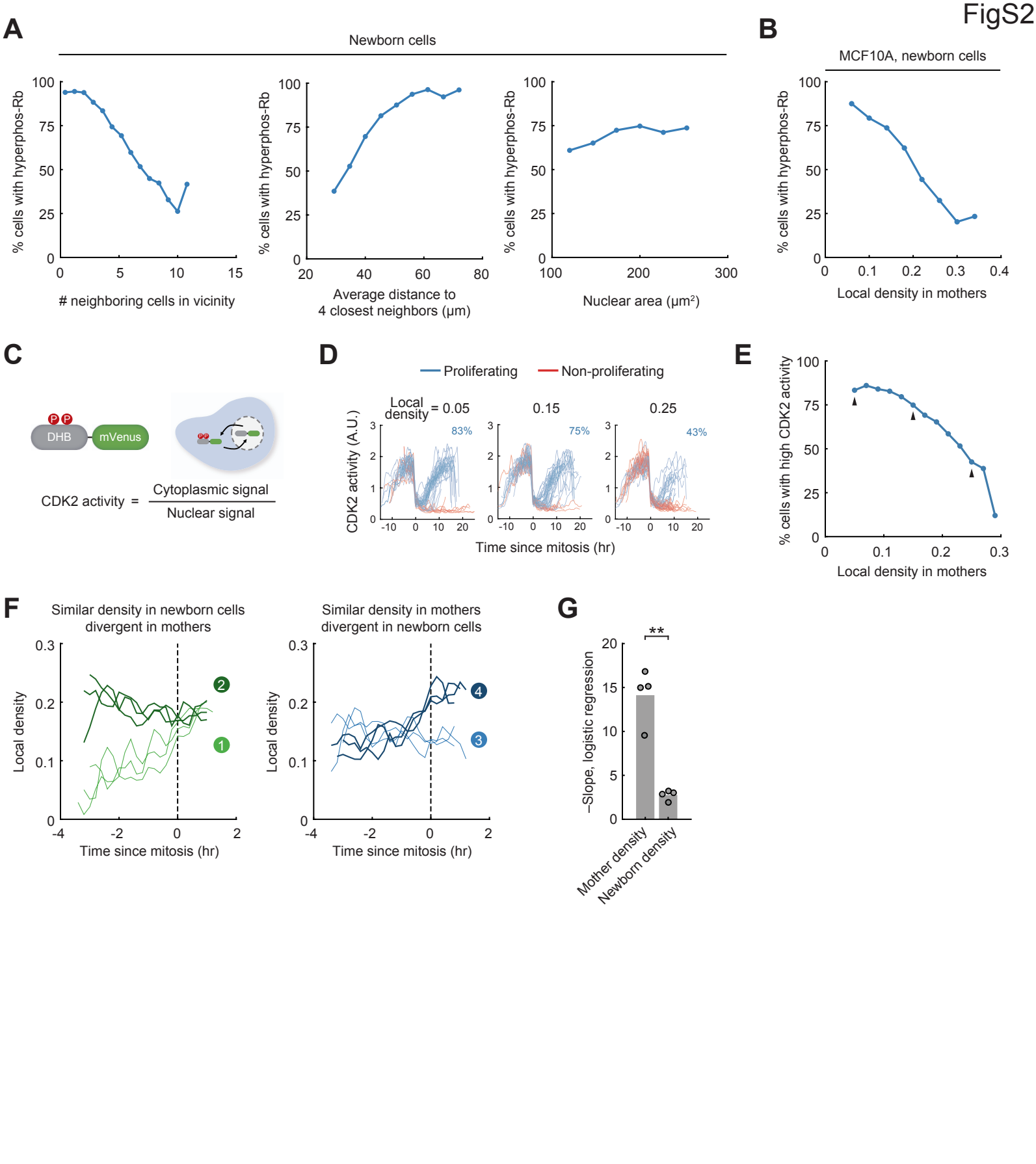
A
Newborn cells
% cells with hyperphos-Rb
# neighboring cells in vicinity
Average distance to 4 closest neighbors (μm)
Nuclear area (μm²)
B
MCF10A, newborn cells
Local density in mothers
C
DHB
mVenus
CDK2 activity = Cytoplasmic signal / Nuclear signal
D
Proliferating
Non-proliferating
Local density = 0.05
0.15
0.25
83%
75%
43%
CDK2 activity (A.U.)
Time since mitosis (hr)
E
% cells with high CDK2 activity
Local density in mothers
F
Similar density in newborn cells divergent in mothers
Similar density in mothers divergent in newborn cells
Local density
Time since mitosis (hr)
G
**
−Slope, logistic regression
Mother density
Newborn density

Figure S2, related to Figure 1

(A) Same experiment as Figure 1E. Correlation between Rb hyperphosphorylation in newborn cells and alternative measures of local cell density in mothers, but not with nuclear area. Logistic regression: slope = -0.45, 0.12, 7.8×10^{-3} ($n \geq 20$ cells per bin, n = 8,574 cells total). Cross-validation (10-fold) was performed on each model: slope = -0.45 ± 0.01, 0.12 ± 0.00, $7.9\times10^{-3} \pm 0.5\times10^{-3}$; AUC-ROC = 0.73 ± 0.02, 0.54 ± 0.03. Data are representative of 4 independent experiments.
(B) MCF10A cells were cultured in serum-free media supplemented with 1 ng/mL EGF. Negative correlation between Rb hyperphosphorylation in newborn cells and local density in mothers. Logistic regression: slope = -14.6; likelihood ratio test, $p = 1.4\times10^{-33}$ ($n \geq 15$ cells per bin, n = 838 cells total). Cross-validation (10-fold) was performed: slope = -14.8 ± 0.3 (median ± s.t.d.), AUC-ROC = 0.73 ± 0.04. Data are representative of 3 independent experiments.

As a second readout of the proliferative status of newborn cells, we used a live-cell reporter that measures cyclin E/A-CDK activity. This reporter primarily measures cyclin E-CDK2 activity during G1 phase (Barr et al., 2017; Chung et al., 2019; Hahn et al., 2009; Schwarz et al., 2018; Spencer et al., 2013; Yang et al., 2020), thus we subsequently refer to the sensor as the CDK2 reporter. CDK2 activity has been shown to bifurcate after mitosis (Moser et al., 2018; Spencer et al., 2013): cells either enter the next cycle by increasing CDK2 activity, or they have low CDK2 activity and exit to quiescence, with some cells activating CDK2 and re-entering the cell cycle after a longer delay (Figure S2D). We measured the effect of local density in mother cells on the CDK2 activity bifurcation in newborn cells, and we again found that the proliferation outcome in newborn cells was predicted by the local cell density experienced by mother cells (Figure S2E).

(C) Schematic of CDK2 activity reporter. DHB is a fragment (aa994-1087) of the human DHB protein. The reporter translocates to the cytoplasm when phosphorylated by cyclin E/A-CDK activity, which is primarily cyclin E-CDK2 activity during G1 (see main text).
(D) Monitoring proliferative state of newborn cells by measuring CDK2 activity. Asynchronously cycling cells expressing H2B-mTurquoise and the CDK2 activity reporter were imaged. Single-cell traces were computationally aligned to the time of mitosis. n = 50 random sample traces of CDK2 activity with varying history of local density in mothers are displayed. Cells were categorized as CDK2-high (proliferating) if CDK2 activity rises above 0.7 after 3 hr post mitosis. Percentages indicate cells with high CDK2 activity in newborn cells.
(E) Same experiment as (D). Newborn cells were binned by the local density experienced by their mothers ($n \geq 25$ cells per bin, n = 10,992 cells total). Arrows indicate data points represented by sample traces. Logistic regression shows that local density in mothers was a strong predictor of CDK2 activity in newborn cells: slope = -12.4; likelihood ratio test, $p = 1.3\times10^{-145}$. Cross-validation (10-fold) was performed: slope = -12.4 ± 0.1 (median ± s.t.d.), AUC-ROC = 0.65 ± 0.01. Data are representative of 2 independent experiments.
(F) Sample traces of local density in each gate outlined in Figure 1F.
(G) Logistic regression model that separates the effects of local density in mothers versus in newborn cells as predictors of Rb hyperphosphorylation in newborn cells. Paired Student's t test, p = 0.0071 (n = 4 independent experiments). Cross-validation (10-fold) was performed on each model: AUC-ROC = 0.74 ± 0.01, 0.72 ± 0.02, 0.71 ± 0.01, 0.67 ± 0.01 (n = 4).

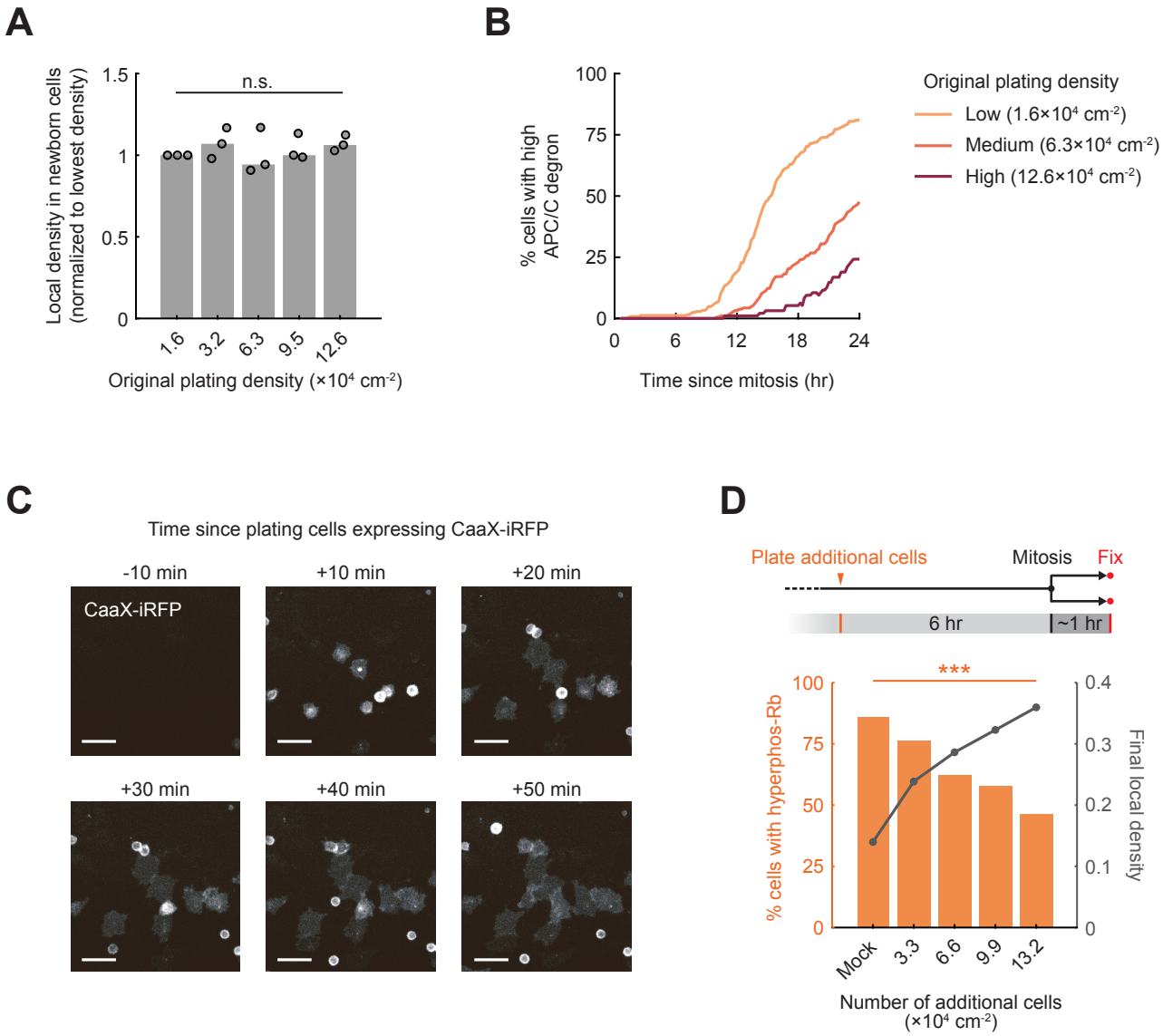
A
Local density in newborn cells (normalized to lowest density)
1.5
1
0.5
0
n.s.
1.6
3.2
6.3
9.5
12.6
Original plating density (×10⁴ cm⁻²)
B
% cells with high APC/C degron
100
75
50
25
0
0
6
12
18
24
Time since mitosis (hr)
Original plating density
Low (1.6×10⁴ cm⁻²)
Medium (6.3×10⁴ cm⁻²)
High (12.6×10⁴ cm⁻²)
C
Time since plating cells expressing CaaX-iRFP
-10 min
+10 min
+20 min
CaaX-iRFP
+30 min
+40 min
+50 min
D
Plate additional cells
Mitosis
Fix
6 hr
~1 hr
***
% cells with hyperphos-Rb
100
75
50
25
0
0.4
0.3
0.2
0.1
0
Final local density
Mock
3.3
6.6
9.9
13.2
Number of additional cells
(×10⁴ cm⁻²)

Figure S3, related to Figure 2

(A) Same experiment as Figure 2A. Cells plated at different densities in 12-well plates were re-plated onto 96-well plates and imaged. Local density was measured in newborn cells and normalized to the lowest plating density ($n \geq 74$ cells per condition). One-way ANOVA, $p = 0.76$ ($n = 3$ independent experiments).
(B) Same experiment as Figure 2B. Cells plated at different densities in 12-well plates were re-plated onto 96-well plates and imaged. Percentage of newborn cells that inactivated APC/C^{Cdh1} and accumulated high levels of the APC/C degron was plotted as a function of time since mitosis ($n \geq 95$ cells per condition). Data are representative of 3 independent experiments.
(C) Cells expressing a cell membrane marker (CaaX-iRFP) were plated onto an existing cell sheet and imaged. Newly plated cells adhered and spread out within 20~30 min. Scale bar: 50 μm.
(D) Top: schematic of experimental setup. Asynchronously cycling cells expressing H2B-mTurquoise were imaged; additional non-fluorescent cells were plated to acutely increase cell density. Bottom: increase in cell density during the mother cell cycle reduced Rb hyperphosphorylation in newborn cells ($n \geq 500$ cells per condition). Data are representative of 4 independent experiments, one-way ANOVA of 4 replicates, $p = 3.1 \times 10^{-4}$.

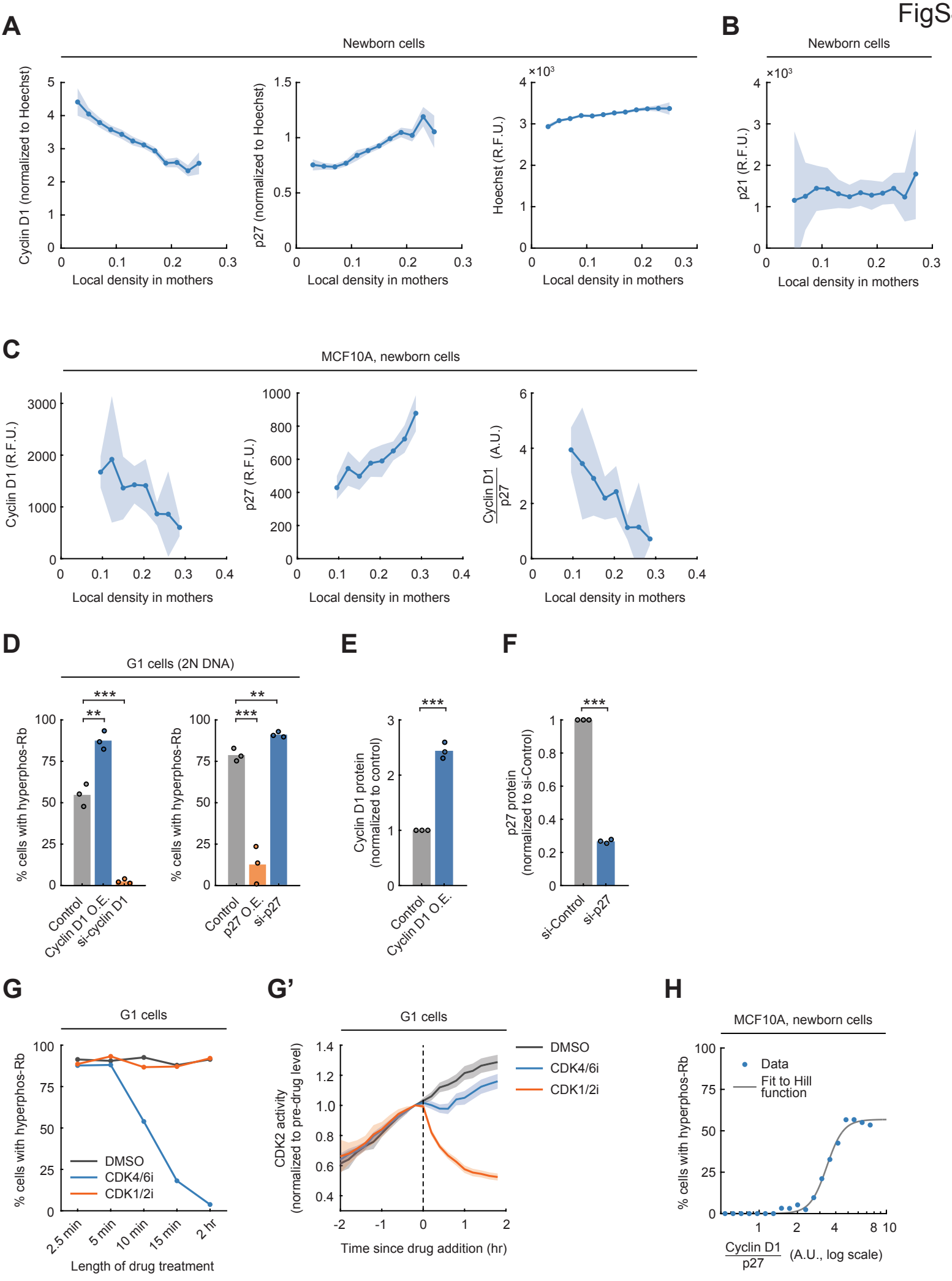
A
Newborn cells
Cyclin D1 (normalized to Hoechst)
p27 (normalized to Hoechst)
Hoechst (R.F.U.)
×10³
Local density in mothers
B
Newborn cells
p21 (R.F.U.)
×10³
Local density in mothers
C
MCF10A, newborn cells
Cyclin D1 (R.F.U.)
p27 (R.F.U.)
Cyclin D1 / p27 (A.U.)
Local density in mothers
D
G1 cells (2N DNA)
% cells with hyperphos-Rb
Control
Cyclin D1 O.E.
si-cyclin D1
p27 O.E.
si-p27
E
Cyclin D1 protein (normalized to control)
F
p27 protein (normalized to si-Control)
si-Control
si-p27
G
G1 cells
DMSO
CDK4/6i
CDK1/2i
Length of drug treatment
G'
G1 cells
CDK2 activity (normalized to pre-drug level)
Time since drug addition (hr)
H
MCF10A, newborn cells
Data
Fit to Hill function
Cyclin D1 / p27 (A.U., log scale)

Figure S4, related to Figure 3

(A) Same experiment as Figure 3A. Cyclin D1 and p27 levels were normalized to Hoechst intensity to account for potential changes in nuclear geometry associated with changes in local density. Cyclin D1: Pearson correlation coefficient = -0.246, $p = 2.7\times10^{-118}$. p27: Pearson correlation coefficient = 0.223, $p = 1.1\times10^{-97}$. Line plots are population medians in each bin; shaded error bars are 95% confidence intervals ($n \geq 50$ cells per bin, n = 8,574 cells total). Data are representative of 4 independent experiments.
(B) No correlation between p21 expression in newborn cells and local density in mothers. Pearson correlation coefficient = -0.033, p = 0.01. Line plots are population medians in each bin; shaded error bars are 95% confidence intervals ($n \geq 60$ cells per bin, n = 5,833 cells total). Data are representative of 2 independent experiments.
(C) MCF10A cells were cultured in serum-free media supplemented with 1 ng/mL EGF. Cyclin D1: Pearson correlation coefficient = -0.248, $p = 1.4\times10^{-4}$. p27: Pearson correlation coefficient = 0.521, $p = 1.7\times10^{-17}$. Cyclin D1/p27 ratio: Pearson correlation coefficient = -0.311, $p = 1.4\times10^{-6}$. Line plots are population medians in each bin; shaded error bars are 95% confidence intervals ($n \geq 13$ cells per bin, n = 225 cells total). Data are representative of 3 independent experiments.
(D) Percentage of G1 cells with Rb hyperphosphorylation was measured one day after over-expression or knock-down. Cyclin D1 or p27 over-expression (O.E.) was driven by a doxycycline-inducible promoter. Control: si-Control + DMSO; O.E.: si-Control + doxycycline; si-cyclin D1/si-p27: siRNA + DMSO. $n \geq 19{,}000$ cells per condition. Student's t test: (i) cyclin D1 O.E. vs control, $p = 2.9\times10^{-3}$; (ii) si-cyclin D1 vs control, $p = 2.0\times10^{-4}$; (iii) p27 O.E. vs control, $p = 6.7\times10^{-4}$; (iv) si-p27 vs control, $p = 6.9\times10^{-3}$.
(E) Same experiment as Figure 3B. Nuclear cyclin D1 protein level (population median), normalized to control. Paired Student's t test, $p = 1.5\times10^{-3}$ (n = 3 independent experiments).
(F) Same experiment as Figure 3C. Nuclear p27 protein level (population median), normalized to si-Control. Paired Student's t test, $p = 3.7\times10^{-4}$ (n = 3 independent experiments).

There are conflicting results on the role and importance of CDK4/6 activity in hyperphosphorylating Rb (Chung et al., 2019; Malumbres and Barbacid, 2001; Narasimha et al., 2014). We tested whether CDK4/6 activity is a rate-limiting step for hyperphosphorylating Rb in newborn RPE-1 cells by using a CDK4/6-selective inhibitor (palbociclib) and a CDK1/2-selective inhibitor (Cdk1/2 Inhibitor III) to acutely inhibit the respective kinase activities, being cognizant that both inhibitors have potential off-target effects. Nevertheless, at the inhibitor concentrations we used, there was only a small effect of the CDK4/6 inhibitor on CDK2 activity measured by the CDK2 reporter, while CDK1/2 inhibitor treatment rapidly suppressed CDK2 activity (Figure S4G'). This allowed us to test the acute effect of the two inhibitors on Rb hyperphosphorylation in G1 cells. We limited the inhibitor treatment to a short time period in order to exclude slow indirect effects reported for long-term palbociclib treatment (Guiley et al., 2019). CDK4/6 inhibitor caused a near-maximal suppression of Rb hyperphosphorylation within 15 minutes, while treatment with the CDK1/2 inhibitor had no significant effect (Figure S4G). These control experiments suggest that activation of CDK4/6 is a rate-limiting step for Rb hyperphosphorylation in newborn RPE-1 cells in G1. A role of CDK4/6 activity in hyperphosphorylating Rb is also consistent with previous results where mouse embryonic fibroblasts still hyperphosphorylated Rb and activated E2F in a CDK4/6 activity-dependent manner when all cyclin E and A genes were deleted (Chung et al., 2019).

(G) Asynchronously cycling cells expressing H2B-mTurquoise, CDK2 activity reporter, and APC/C degron reporter were treated with DMSO, CDK4/6 inhibitor (palbociclib, 1 μM), or CDK1/2 inhibitor (Cdk1/2 Inhibitor III, 1 μM) for the indicated amount of time. Newborn cells in G1 (low APC/C degron) were gated *in silico* for analysis. $n \geq 90$ cells per condition. Fisher's exact test comparing DMSO vs CDK4/6i treatment for 15 min: $p = 2.4\times10^{-24}$; comparing DMSO vs CDK1/2i treatment for 15min: p = 1. Data are representative of 2 independent experiments.
(G') Same experiment as (G). Cells in G1 (low APC/C degron) and with CDK2 activity between 0.7 and 0.9 were gated *in silico* for analysis. CDK2 activity was normalized to the frame before drug treatment.

Line plots are population medians of $n \geq 89$ cells; shaded error bars are 95% confidence intervals. Student's t test comparing non-normalized CDK2 activity in DMSO vs CDK1/2i: 12 min before drug treatment, $p = 0.21$; 1 hr after drug treatment, $p = 4.7\times10^{-54}$. Student's t test comparing non-normalized CDK2 activity in DMSO vs CDK4/6i: 12 min before drug treatment, $p = 0.79$; 1 hr after drug treatment, $p = 1.2\times10^{-5}$. Data are representative of 2 independent experiments.
(H) MCF10A cells were cultured in serum-free media supplemented with 3 ng/mL EGF. Percentage of newborn cells with Rb hyperphosphorylation is plotted as a function of cyclin D1/p27 ratio ($n \geq 18$ cells per bin, $n = 776$ total). Hill coefficient = 6.9 ± 1.6 (mean ± s.t.d. of 3 independent experiments).

FigS5

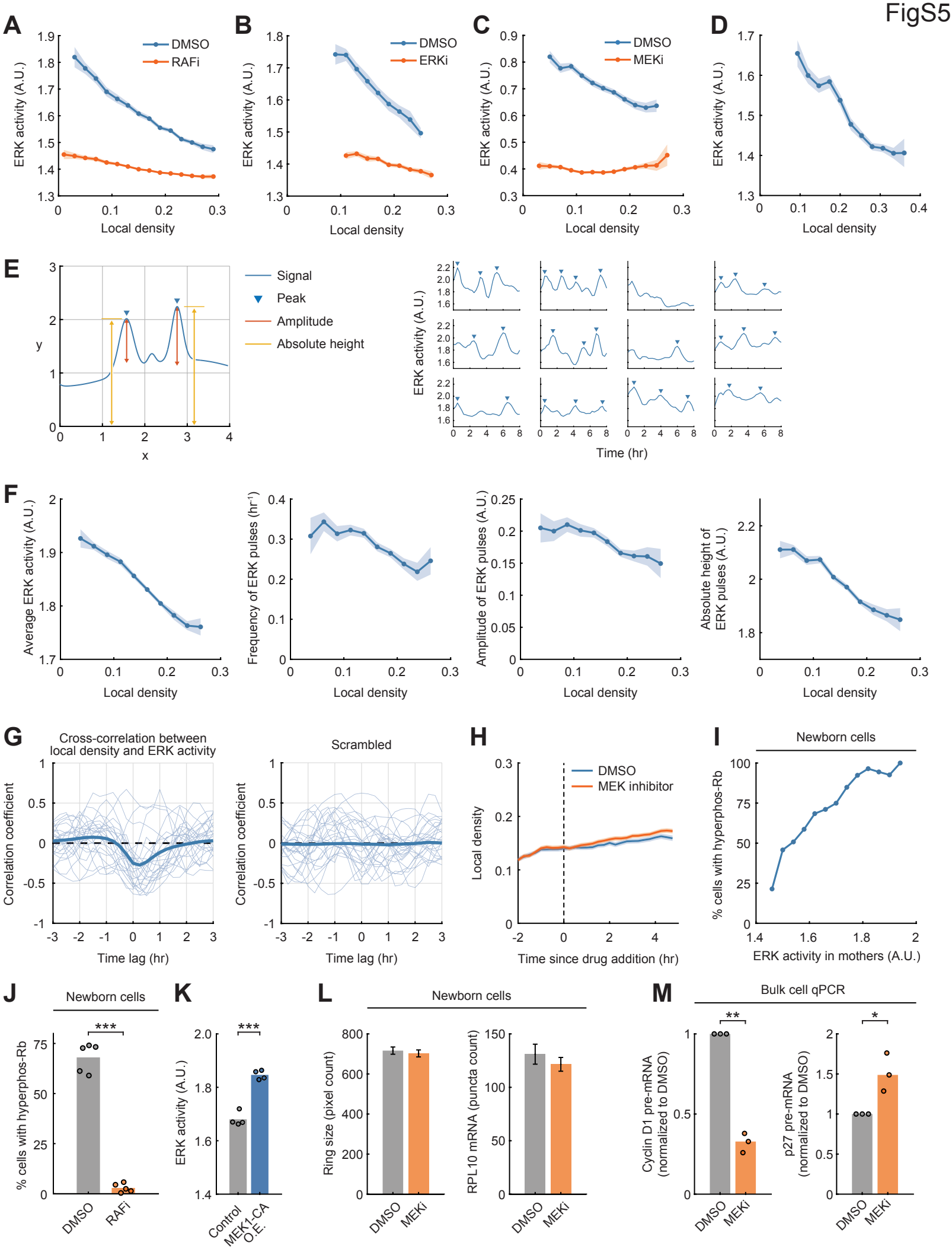
A
DMSO
RAFi
ERK activity (A.U.)
Local density
B
DMSO
ERKi
ERK activity (A.U.)
Local density
C
DMSO
MEKi
ERK activity (A.U.)
Local density
D
ERK activity (A.U.)
Local density
E
Signal
Peak
Amplitude
Absolute height
y
x
ERK activity (A.U.)
Time (hr)
F
Average ERK activity (A.U.)
Frequency of ERK pulses (hr⁻¹)
Amplitude of ERK pulses (A.U.)
Absolute height of ERK pulses (A.U.)
Local density
G
Cross-correlation between local density and ERK activity
Scrambled
Correlation coefficient
Time lag (hr)
H
DMSO
MEK inhibitor
Local density
Time since drug addition (hr)
I
Newborn cells
% cells with hyperphos-Rb
ERK activity in mothers (A.U.)
J
Newborn cells
% cells with hyperphos-Rb
***
DMSO
RAFi
K
ERK activity (A.U.)
***
Control
MEK1-CA O.E.
L
Newborn cells
Ring size (pixel count)
RPL10 mRNA (puncta count)
DMSO
MEKi
M
Bulk cell qPCR
Cyclin D1 pre-mRNA (normalized to DMSO)
p27 pre-mRNA (normalized to DMSO)
**
*
DMSO
MEKi

Figure S5, related to Figure 4

(A) Negative correlation between ERK activity (time-averaged over 2 hr) and local density. RAF inhibitor: LY3009120, 4.096 μM. Linear regression slope = -1.19 vs -0.32. Line plots are population medians in each bin; shaded error bars are 95% confidence intervals ($n \geq 22$ cells per bin, DMSO: n = 3,123 cells total, RAFi: n = 4,580 cells total). Data are representative of 3 independent experiments.
(B) Negative correlation between ERK activity (time-averaged over 2 hr) and local density. ERK inhibitor: SCH772984, 1 μM. Linear regression slope = -1.54 vs -0.42. Line plots are population medians in each bin; shaded error bars are 95% confidence intervals ($n \geq 36$ cells per bin, DMSO: n = 632 cells total, ERKi: n = 902 cells total). Data are representative of 3 independent experiments.
(C) Negative correlation between ERK activity (measured by ERK-KTR, time-averaged over 3 hr) and local density. MEK inhibitor: PD0325901, 100 nM. Linear regression slope = -0.93 vs 0.12. Line plots are population medians in each bin; shaded error bars are 95% confidence intervals ($n \geq 42$ cells per bin, DMSO: n = 1,737 cells total, MEKi: n = 2,352 cells total).
(D) MCF10A cells were cultured in serum-free media supplemented with 1 ng/mL EGF. Negative correlation between ERK activity (time-averaged over 4 hr) and local density. Pearson correlation coefficient = -0.55. Shaded error bars are 95% confidence intervals ($n \geq 25$ cells per bin, n = 1,686 cells total). Data are representative of 3 independent experiments.
(E) Left: schematic of ERK pulse detection using MATLAB's findpeaks function, which finds the local maxima. Peaks with width > 1.3 frames (~20 min) and amplitude > 0.08 were called. Right: sample traces of ERK activity and detected peaks.
(F) Negative correlation between ERK activity (time-averaged and pulse properties measured over the course of 8 hr) and local density. Pearson correlation coefficient, time average: -0.64, pulse frequency: -0.254, pulse amplitude: -0.189, pulse height: -0.487. Shaded error bars are 95% confidence intervals ($n \geq 36$ cells per bin, n = 2,475 cells total). Data are representative of 3 independent experiments.
(G) Left: temporal cross-correlation between local density and ERK activity (dark line shows population median of n = 977 cells, light lines are 25 random samples). Right: cross-correlation when cells were randomly scrambled. Data are representative of 3 independent experiments.
(H) Local cell density after inhibition of MEK activity (PD0325901, 100 nM) ($n \geq 259$ cells). Student's t test comparing ERK activity in DMSO vs MEK inhibitor: 15 min before release, p = 0.43; 30 min after release, p = 0.12. Data are representative of 3 independent experiments.
(I) ERK activity in mother cells (time-averaged during -5 hr ~ -3 hr relative to mitosis) was a strong predictor of Rb hyperphosphorylation in newborn cells. Logistic regression: slope = 8.9; likelihood ratio test, $p = 4.2\times10^{-52}$ ($n \geq 14$ cells per bin, n = 2,026 cells total). Cross-validation (10-fold) was performed: slope = -8.9 ± 0.2 (median ± s.t.d.), AUC-ROC = 0.72 ± 0.03. Data are representative of 3 independent experiments.
(J) Inhibition of the MEK-ERK pathway (7h treatment with RAFi: LY3009120, 4.096 μM) blocked Rb hyperphosphorylation in newborn cells ($n \geq 617$ cells per condition). Student's t test, $p = 5.8\times10^{-8}$ (n = 5 independent experiments).
(K) Same experiment as Figure 4F. Cells expressing the construct, as measured by immunofluorescence signal of HA-tagged MEK1-CA, were gated *in silico* for analysis. ERK activity in mother cells was time-averaged during -5 hr ~ -3 hr relative to mitosis. Student's t test, $p = 4.2\times10^{-5}$ (n = 3 independent experiments).
(L) Same experiment as Figure 4G. Cytoplasmic ring size (used for counting FISH puncta) and an unrelated mRNA *RPL10* were largely unaffected by MEK inhibition. Error bars are 95% confidence intervals. Kolmogorov-Smirnov test, cytoplasmic ring size: p = 0.64, RPL10 mRNA: p = 0.023 (DMSO: n = 324 cells, MEK inhibitor: n = 390 cells). Data are representative of 3 independent experiments.
(M) Short-term inhibition of MEK activity (1h treatment with MEKi: PD0325901, 100 nM) reduced nascent cyclin D1 mRNA transcription and increased nascent p27 mRNA transcription, as measured by RT-qPCR using primers that amplify intronic regions. Student's t test, cyclin D1 $p = 4.9\times10^{-3}$, p27 p = 0.019 (n = 3 independent experiments).

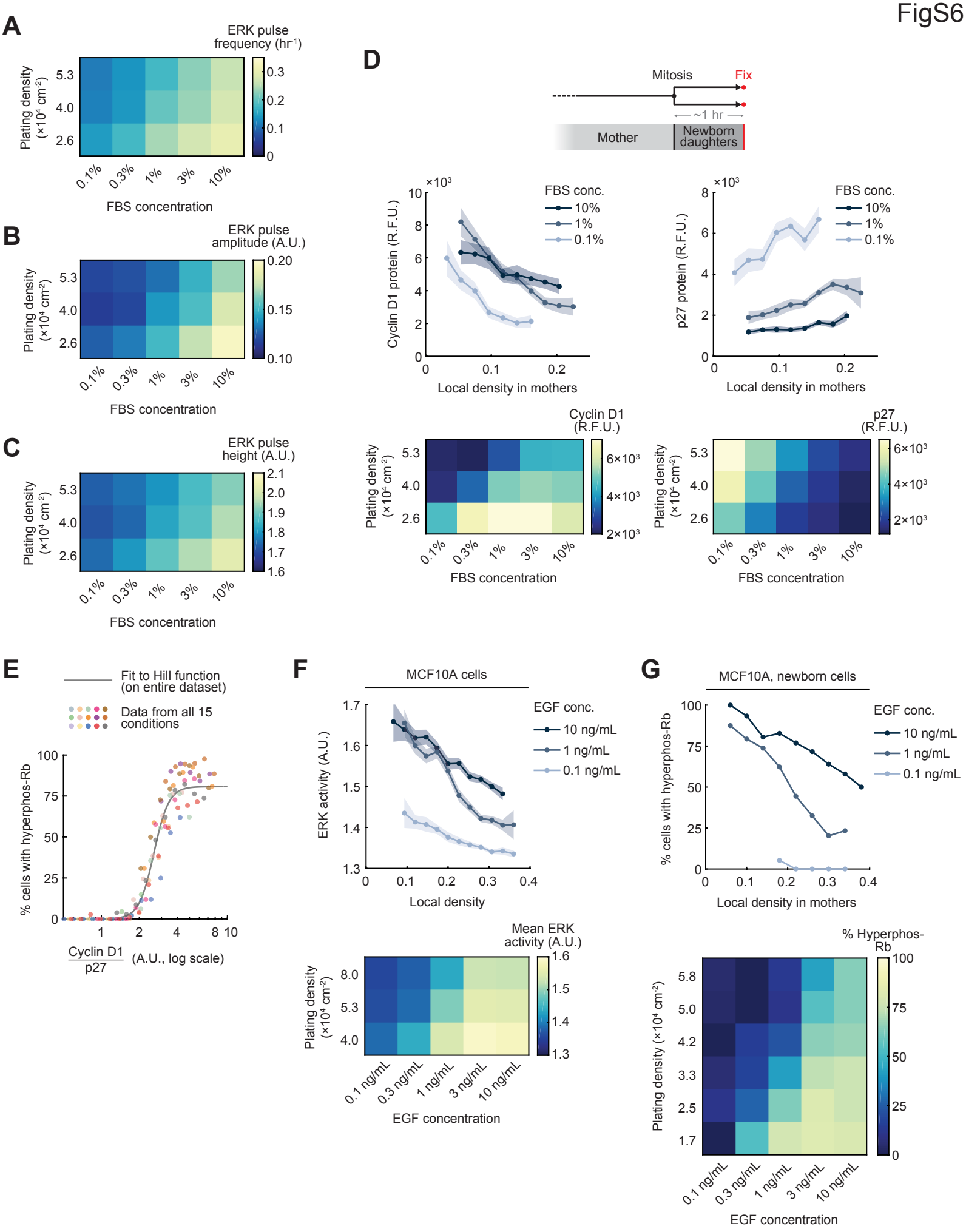
A
ERK pulse frequency (hr-1)
Plating density (×10⁴ cm⁻²)
5.3
4.0
2.6
0.3
0.2
0.1
0
0.1%
0.3%
1%
3%
10%
FBS concentration
B
ERK pulse amplitude (A.U.)
0.20
0.15
0.10
C
ERK pulse height (A.U.)
2.1
2.0
1.9
1.8
1.7
1.6
D
Mitosis
Fix
~1 hr
Mother
Newborn daughters
Cyclin D1 protein (R.F.U.)
p27 protein (R.F.U.)
×10³
FBS conc.
10%
1%
0.1%
Local density in mothers
Cyclin D1 (R.F.U.)
p27 (R.F.U.)
6×10³
4×10³
2×10³
E
Fit to Hill function (on entire dataset)
Data from all 15 conditions
% cells with hyperphos-Rb
Cyclin D1 / p27 (A.U., log scale)
F
MCF10A cells
ERK activity (A.U.)
EGF conc.
10 ng/mL
1 ng/mL
0.1 ng/mL
Local density
Mean ERK activity (A.U.)
0.1 ng/mL
0.3 ng/mL
1 ng/mL
3 ng/mL
10 ng/mL
EGF concentration
G
MCF10A, newborn cells
% Hyperphos-Rb

Figure S6, related to Figure 5

(A) ~ (C) Same experiment as Figure 5A, except ERK activity was analyzed as pulses (measured over the course of 8 hr). Population medians of ERK pulsing properties ($n \geq 330$ cells per condition). Data are representative of 3 independent experiments.
(D) Measuring the effect of opposing cell density and mitogen signals on cyclin D1 and p27 expression. Top: schematic for experimental setup. Middle: line plots are population medians of $n \geq 30$ cells per bin; shaded error bars are 95% confidence intervals. Bottom: population medians of cyclin D1 and p27 expression levels ($n \geq 250$ cells per condition). Data are representative of 3 independent experiments.
(E) Determining whether opposing cell density and mitogen signals converge onto the same activator-inhibitor balance. Same experiment as Figure 6B. Percentage of newborn cells with Rb hyperphosphorylation is plotted as a function of cyclin D1/p27 ratio ($n \geq 20$ cells per bin). Hill curve was fitted to the entire dataset. Note that for each condition, bin boundaries were slightly shifted by a small random amount to facilitate visualization by avoiding a large number of overlapping points. As a result, data points in Figure 5C and S6E may not appear identical.
(F) Top: mitogen levels and local cell density had opposite and dose-dependent effects on ERK activity in MCF10A cells ($n \geq 20$ cells per bin, shaded error bars are 95% confidence intervals). Bottom: population medians of ERK activity ($n \geq 283$ cells per condition). Data are representative of 3 independent experiments.
(G) Top: mitogen levels and local density in mothers had opposing effects on Rb hyperphosphorylation in newborn MCF10A cells ($n \geq 11$ cells per bin, shaded error bars are 95% confidence intervals). Bottom: percentage of cells with hyperphosphorylated Rb ($n \geq 8$ cells per condition). Data are representative of 3 independent experiments.